Front. Optoelectron. China 2011, 4(1): 65–71
DOI 10.1007/s12200-011-0204-3

RESEARCH ARTICLE

# Enhanced electron injection/transportation by surface states increment in mesoporous $TiO_2$ dye-sensitized solar cells

**Minghui DENG[1], Shuqing HUANG[1], Zhexun YU[1], Dongmei LI[1], Yanhong LUO[1], Yubai BAI[2], Qingbo MENG (✉)[1]**

1 Beijing National Laboratory for Condensed Matter Physics, Institute of Physics, Chinese Academy of Sciences, Beijing 100190, China
2 College of Chemistry, Jilin University, Changchun 130023, China



**Abstract** A strategy of surface modification to the mesoporous $TiO_2$ photoanode with hydrochloric acid treatment was used in this study, and it was found that short circuit current and photovoltaic efficiency of dye-sensitized solar cells (DSSCs) were increased by 5.5% and 8.9% respectively. The improvement was attributed to the reduced impedances in the $TiO_2$ film and at the $TiO_2$/dye/electrolyte interface. It was showed that the increased surface electronic states could remarkably prolong electron lifetime, which was responsible for the reduction of impedances. Under these quasi-continuous states in mesoporous structure, the electron injection/transportation can be notably facilitated, which will be beneficial for the DSSC performance.

**Keywords** dye-sensitized solar cell (DSSC), surface states, surface modification, electron transportation

## 1 Introduction

Dye-sensitized solar cells (DSSCs) have been under intensive investigations since Prof. Grätzel contributed a respectable innovation for photovoltaic performance by introducing the mesoporous $TiO_2$ film as photoanode [1–11]. With the introduction of porous structure, dye molecules loading area and redox electrolyte contacting interface on $TiO_2$ film are increased in magnitude for several orders compared to plain ones [1,2]. The resulting enhancement in light absorption greatly improves cell efficiency and makes great strides for the practical application of DSSCs. Consequently, in order to further optimize DSSCs performance, great efforts have been devoted to $TiO_2$ film surface modification strategies [12–22]. Briefly, these modification methods can be summarized into two classes: 1) the blocking ones, which mainly aim at suppressing electron loss on film surface. The generally adopted approach is depositing an insulating oxide layer outside the nanoparticles by chemical or physical approach [19–22]; 2) the boosting ones, which include the methods trying to promote dye adsorption, electron injection, carrier transportation and collection [12–18]. Among these boosting methods, hydrochloric acid treatment of $TiO_2$ photoanode is a simple and effective approach [15–18], and the main effect is to enhance photocurrent. On the other hand, when boosting strategy concerning charge transportation is considered, the abundant surface electronic states are always mentioned [2,3,8]. These surface states are customarily deemed to be trapping sites for photoinjected electrons in DSSCs, slowing down the charge transport and sometimes become recombination centers [3,8,9,13]. However, recent studies indicate that the influence of surface states seems to be more than just detention. With appropriate modulation approaches, former trapping states can also be helpful for electron transportation. Under ultraviolet (UV) illumination, Gregg et al. reported that a high concentration of photoactive surface states created in the mesoporous $TiO_2$ films could improve photoinjection and carrier transportation, and they improved the efficiency for 12.8% [12]. Another paper published by Grätzel et al. also proved that electronic transport levels close to the conduction band arisen from visible light-soaking increased photovoltaic performance for 2.9% [14]. These findings pioneer a new path to elevate DSSCs efficiency through adjusting electronic states in mesoporous $TiO_2$ by designing the film surface modification strategy. Unsatisfactorily, there is a common limitation for above irradiation methods — the widely used $Li^+$ ions in electrolyte will hinder the formation of the transport states [13,14]. Therefore,

Received October 18, 2010; accepted December 30, 2010

E-mail: qbmeng@aphy.iphy.ac.cn

seeking an ideal method to create transporting states insensitive to certain ingredients in electrolyte is in urgent need now.

Here we fabricated DSSCs by using $TiO_2$ photoanodes which were treated with aqueous hydrochloric acid and following sintering procedure. Measurement results under various illumination intensities confirm the treatment to be beneficial all the time with electrolyte containing $Li^+$ ions. After characterizations with UV-Vis spectroscopy, electrochemical impedance spectroscopy (EIS) and X-ray photoelectron spectroscopy (XPS), we demonstrate that the improved photocurrent of HCl modified DSSC is attributed to the added states brought by surface hydroxyl groups, leading to the facilitation of electron injection and transportation in photoanode. These results show that modification in electronic states of mesoporous $TiO_2$ surface can be of critical importance in the future development of DSSCs.

## 2 Experiment

### 2.1 $TiO_2$ electrode preparation and cell fabrication

DSSCs were fabricated as follows. Degussa P25 paste was deposited on FTO conducting glass ($5\ \Omega\cdot sq^{-1}$) by screen-printing method, followed by sintering at 450°C for 30 min (normal anode). The film was then dipped in 0.5 M aqueous hydrochloric acid under room temperature for 1 h and dried by $N_2$ flow before it was sintered again at 450°C for 30 min (modified anode). All $TiO_2$ anodes were immersed in dry ethanol solution of dye N3 (Solaronix) with a concentration of 0.3 mM overnight. The redox electrolyte was composed of 0.1 M LiI, 0.05 M $I_2$, 0.6 M methylhexylimidazolium iodide, and 0.5 M 4-tert-butylpyridine in 3-methoxypropionitrile. The DSSC was fabricated in air by clamping the sensitized $TiO_2$, a drop of electrolyte and a platinized ITO counter electrode with two clips. The active electrode area for each cell was 0.15 $cm^2$. DSSCs with different anodes are denoted as normal cell and modified cell in the following.

### 2.2 Photovoltaic measurement and characterization

Current-photovoltage characteristics were recorded under simulated AM1.5 irradiation (Oriel, 91192) in the air for DSSCs. The weakened intensity measurements were realized by inserting neutral density filter between the light source and tested cell. All measurements were recorded by a potentiostat (Princeton Applied Research, Model 263A). UV-Vis absorption spectra measurements were conducted with UV-Vis spectrophotometer (Shimadzu, Model 2550) for sensitizer dissolved into 0.1 M NaOH solution from dye-loaded normal and modified films. EIS measurements were carried out on electrochemical workstations (Zahner, IM6ex) for illuminated DSSCs as mentioned above. The frequency scanning range is $10^{-1}$–$10^5$ Hz. The DSSCs were biased with open circuit voltage under a sinusoidal perturbation of 10 mV. Corresponding equivalent circuit simulation and data fitting were performed with software equipped to the workstations (Zahner, Thales). XPS measurements were performed on MKII spectrometer (VG, UK) for freshly made normal and modified $TiO_2$ anodes, with X-ray source $Mg_{Ka}$ = 1253.6 eV. A sample area of 2 mm × 2 mm was analyzed with pass energy of 50 eV. Binding energy was calibrated by $C_{1s}$ = 284.6 eV.

## 3 Results and discussion

### 3.1 Cell performance

Figure 1 shows the performances of normal and modified DSSCs under various illumination intensities. The linear dependence of short circuit current density ($J_{sc}$) on the illumination is in good agreement with expectation. Obvious enhancements in $J_{sc}$ and cell efficiency ($\eta$) are observed all over the 25, 50, 75, 100 $mW\cdot cm^{-2}$ light intensities, but the open circuit voltage ($V_{oc}$) and fill factor ($FF$) only show slight changes. For comparison, HCl treated anodes without sintering process are also tested, but they are not so effective for DSSCs performance as the sintered ones. Under illumination of simulated AM 1.5 (100 $mW\cdot cm^{-2}$), $J_{sc}$ and $\eta$ increase 5.5% and 8.9% after HCl treatment, respectively. Therefore, the improvement for $\eta$ is ascribed mainly to the result of improvement in $J_{sc}$.

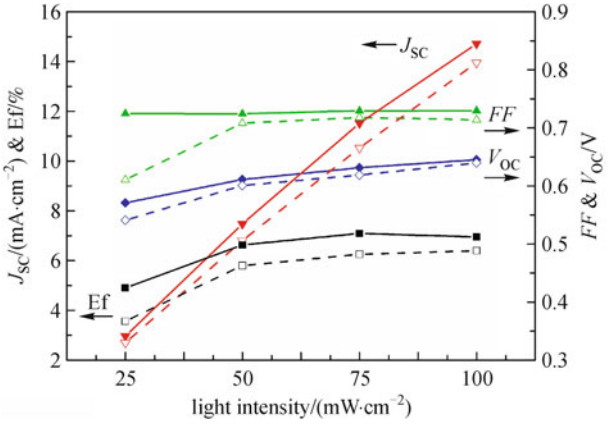


**Fig. 1** Cell performance for normal (dash line) and modified (solid line) DSSCs under various illumination intensities

### 3.2 Light harvesting

There are many processes involved for the determination of $J_{sc}$, including light absorption by sensitizer, electron injection into $TiO_2$ conduction band ($E_c$) from activated dye molecule, carrier transportation in mesoporous film

and electron recombination with oxidative $I_3^-$ in electrolyte [19], thus the treatment may affect one or more of the above processes. UV-Vis absorption spectra of N3 solution desorbed from both samples are shown in Fig. 2. Absorbance through the whole wavelength scale reveals no remarkable distinction. The absorbance at 510 nm due to metal-to-ligand charge transfer (MLCT) is chosen for evaluating amount of absorbed dye molecules and the calculated results are $6.93 \times 10^{-8}$ and $7.03 \times 10^{-8}$ mol·cm$^{-2}$ for normal and modified anodes. The difference is only about 1%, indicating that the modification actually doesn't alter the dye loading amount.

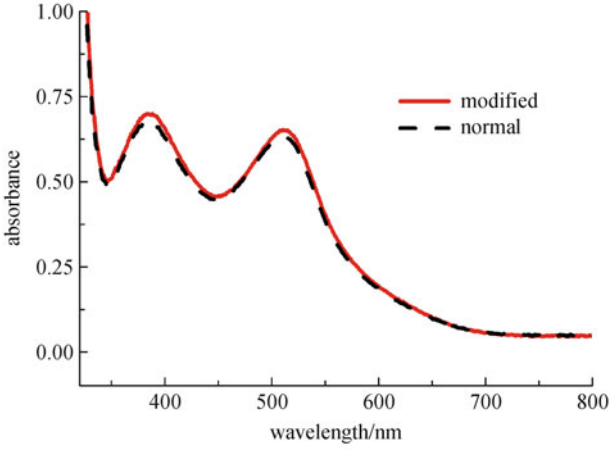


**Fig. 2** Absorption spectra of desorbed sensitizer solution of normal (dash line) and surface modified (solid line) $TiO_2$ photoanodes

In previous reports about HCl treatment effect, significant enhancements in dye adsorption for self-synthesized $TiO_2$ were shown as the main reason for $J_{sc}$ increase and the cause was usually attributed to $H^+$ ions adsorbed on $TiO_2$ surface [15,16], which meanwhile brought disturbing problems like dye selectivity and photovoltage decrease [15]. However, it is not able to get the significantly enhanced absorbance in present study. Since the chemical bonding of N3 on $TiO_2$ nanoparticle is very sensitive to the surface chemistry, which strongly depends on the $TiO_2$ synthesis routes [23,24], the different sources of nanocrystal $TiO_2$ used to fabricate photoanode should account for the various responses of dye loading amount to the acid treatment. Considering the extensive availability and abundant productivity, the characteristics exhibited by P25 are certainly of more practical significance.

### 3.3 Surface structure

Surface structure plays an important role in determining DSSCs performance, because chemically or physically adsorbed molecules and groups on film surface are crucial for the film property. Here, investigation by XPS measurement is adopted to identify the physical origin of $J_{sc}$ enhancement. As shown in Fig. 3, the dominant peak with binding energy of 530 eV is ascribed to oxygen in $TiO_2$.

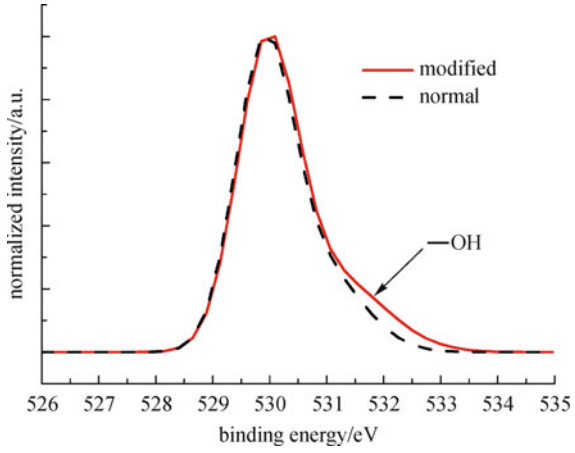


**Fig. 3** Normalized O (1 s) XPS spectra of freshly made normal (dash line) and modified (solid line) $TiO_2$ photoanodes

Measurement data reveals that the mole ratio of O:Ti rises from 2.53 to 2.57 after HCl modification, indicating an increment of oxygen atoms on surface. This increment is explicitly confirmed by the shoulder peak enhancement at 532 eV, which is attributed to the presence of hydroxyl groups [18]. The intensity enhancement in hydroxyl peak is the direct influence of HCl modification and these additional hydroxyl groups are usually supposed to be the cause of electronic states on the film surface [14]. Also worth mention that there is no detectable element $C_l$ in the $TiO_2$ film by XPS, indicating the treatment brings no $C_l$ into the film.

### 3.4 Electronic property

Electron transportation in DSSC is a complicated process involving charge exchange at several interfaces, but luckily it can be probed by the widely recognized EIS measurement [25–27]. EIS measurements for DSSC can be conducted under various conditions, depending on the investigation purpose. To study the electronic property at the $TiO_2$/dye/electrolyte interface, the DSSCs were biased toward $V_{oc}$ for three advantages: 1) there is no current throughout the cell, thus only the current due to perturbation voltage can be flowing in the cell, and this will get rid of the disturbances brought by background current. Consequently the results can show the response of DSSC accurately; 2) under this circumstance, Faradaic processes (processes that involve electron transfer) dominate on the charge transfer electrode — $TiO_2$ photoanode, ensuring the EIS results reveal actual process of electron exchange between the $TiO_2$ and electrolyte, which made

the interface process simple and our equivalent circuit appropriate; 3) when the DSSC is applied with $V_{oc}$, the Fermi level of transparent conductive oxide layer is in alignment with that of $TiO_2$, thus the factor like resistance at the FTO/$TiO_2$ interface is neglectable. Distinct alterations of the Nyquist plots for normal and modified cells under different irradiation conditions were illustrated in Fig. 4(a). The impedance is clearly reduced in modified cells under all illumination conditions, in agreement with the $J_{sc}$ enhancement shown in Fig. 1. For further elucidation of the changes after HCl modification, an equivalent circuit is proposed in Fig. 4(b) to simulate the interface characteristic within the cell [25].

Three parts of the equivalent circuit represent the impedance of Pt/electrolyte interface (subscript 1), $TiO_2$/dye/electrolyte interface (subscript 2) and series resistance (subscript s, including resistance in $TiO_2$ film and electrolyte). The symbols $R$ and $C$ describe a resistance and a capacitance respectively; $Z$ accounts for finite-length Warburg diffusion and $CPE$ stands for the constant phase element. The resistance depicts how difficult for electrons to get across such an interface and capacitance reveals the volume of available electronic states there. Table 1 shows detailed fitting values of all circuit elements. Notably, $R_1$ and $R_2$ at two interfaces reversely depend on illumination intensity, while series resistance $R_s$ is much more retarded to light intensity. Choosing the independent $R_s$ is thus more direct and accurate in reflecting the HCl treatment effect on $TiO_2$ surface. After the modification, average $R_s$ decreases about 30% from 13.70 to 10.13 Ω. Since the value contains resistance from both $TiO_2$ film and electrolyte, with the latter identical for two samples, better carrier transportation is confirmed in the modified sample.

Derived from fitting values in Table 1, Fig. 5(a) illustrates the dependence of $TiO_2$/dye/electrolyte interface resistance log ($R_2$) on $V_{oc}$. Obvious reduction in $R_2$ suggests greater transfer probability for electron injecting from excited sensitizer to $TiO_2$ film after modification.

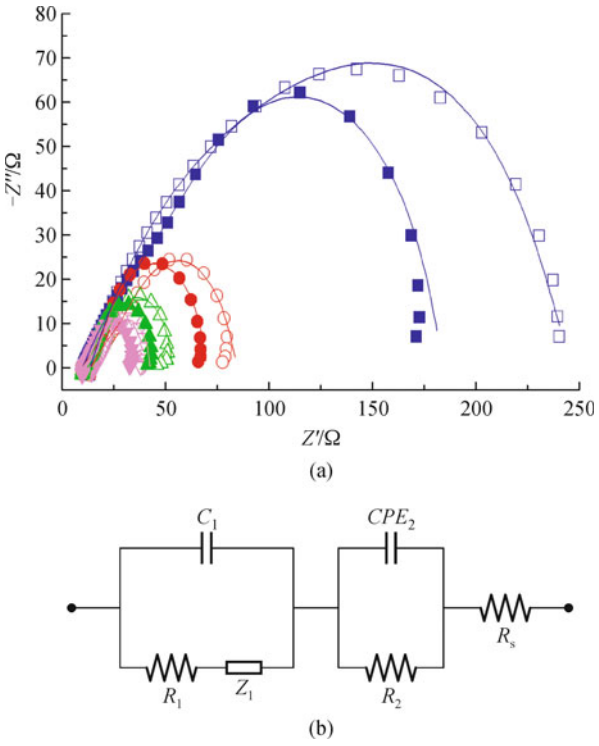


**Fig. 4** (a) Nyquist diagram of experiment (scatter) and the fitting curve (line) of impedance spectra obtained for normal (hollow) and acid pretreated (solid) DSSCs under different light intensities (▽: 100%; △: 75%; ○: 50%; □: 25%); (b) equivalent circuit for EIS spectra simulation

Generally, the charge transfer probability ($P$) at $TiO_2$/dye/electrolyte interface can be described by

$$P \propto n_e N_s, \tag{1}$$

where $n_e$ and $N_s$ represent the excited electrons density from sensitizer and trapping sites on the $TiO_2$ surface respectively. With constant excited electrons density (based on the fact that the amount of dye molecules

**Table 1** Fitting values of measured electrochemical impedance spectra with equivalent circuit in Fig. 4(b)

| samples under different light intensities | $R_1$/Ω | $Z_1$/(mΩ·s$^{-1}$) | $C_1$/mF | $CPE_2$ | | $R_2$/Ω | $R_s$/Ω |
|---|---|---|---|---|---|---|---|
| | | | | $C_2$/ μF | $n$ | | |
| normal-25% | 54.05 | 350.7 | 1.031 | 16.37 | 0.6348 | 177.8 | 13.69 |
| normal-50% | 36.29 | 16.38 | 1.113 | 31.97 | 0.5002 | 35.32 | 13.96 |
| normal-75% | 28.33 | 2.292 | 1.082 | 44.35 | 0.4903 | 13.14 | 12.27 |
| normal-100% | 20.01 | 1.261 | 1.179 | 57.32 | 0.4785 | 7.957 | 14.86 |
| HCl-25% | 91.96 | 6.446 | 0.8311 | 23.68 | 0.563 | 83.14 | 10.05 |
| HCl-50% | 41.73 | 1.097 | 0.9719 | 43.46 | 0.4896 | 18.53 | 10.11 |
| HCl-75% | 25.71 | 0.893 | 1.119 | 57.88 | 0.477 | 9.499 | 10.15 |
| HCl-100% | 18.22 | 0.8793 | 1.259 | 75.64 | 0.4882 | 7.059 | 10.21 |

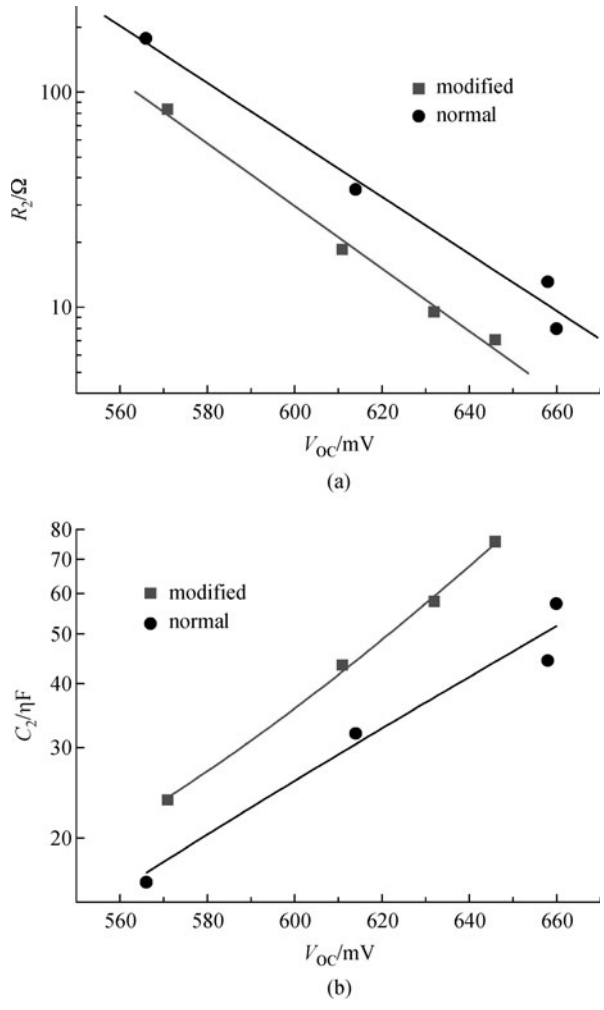


**Fig. 5** $TiO_2$/dye/electrolyte interface property dependence on $V_{oc}$ with logarithm coordinates in vertical. (a) Resistance; (b) capacitance

adsorbed on $TiO_2$ stays unchanged), larger $N_s$ is predicted by greater $P$, which means more locating sites in the film are created after HCl modification and the injection of electrons at the $TiO_2$/dye/electrolyte interface is significantly facilitated.

Notably another characteristic in the Fig. 5(a) is the linearity of log ($R_2$) versus $V_{oc}$, revealing the diode characteristic at the interface. Thus Eq. (2) is used to describe the relationship between $R_2$ and $V_{oc}$:

$$R \propto \exp\left(-\frac{qV}{nk_BT}\right), \tag{2}$$

where $q$, $V$ and $n$ are elementary charge, voltage, and ideality factor respectively [26]. After data fitting, 1.26 and 1.15 were obtained for $n$ in normal and HCl treated DSSCs. According to PN junction principles in semiconductor physics, the smaller ideality usually represents a more ideal diode and less carrier loss in the device. Consequently, improved $TiO_2$/dye/electrolyte interface characteristic after modification is verified again.

Figure 5(b) shows log ($C_2$) dependence on $V_{oc}$. The interface capacitance is thought to be composed of different sections, including the electronic states, the Helmholtz layer and the adsorbed ionic species, but the first one is dominant of all when the potential is high [27]. Enlarged $C_2$ value in Fig. 5(b) is consistent with the above prediction of increased electron states $N_s$ in $TiO_2$. Assuming an exponential distribution of surface states below the $E_c$, the density of surface states can be expressed in the form of Eq. (3) [14]:

$$g_s(E) = \frac{\alpha N_L}{k_BT}\exp\left[\frac{\alpha(E-E_c)}{k_BT}\right], \tag{3}$$

where $N_L$ is the total density of localized states and $\alpha$ is a coefficient that denotes the distribution of surface states; $k_B$ and $T$ are Boltzmann constant and temperature. Based on the slopes of two fitting lines in Fig. 5(b), $\alpha$ is calculated to be 0.28 and 0.5 for normal and HCl treated cell respectively, indicating the narrowing of distribution for surface states in modified cell. In contrast with the conclusion in a previous report [14], where electronic states distributed wider after light-soaking; here the surface states distributed in a narrower energy range. This can be inferred by considering the locations of these states: light-soaking increases density of deeper traps in the bulk, but present treatment brings shallow traps at film surface. Since more surface shallow trapping sites spread in a narrower energy region, it will arouse higher density of surface electronic states in the film. In principle, carriers in the $TiO_2$ mesoporous structure usually follow a trapping-detrapping transporting pattern [28,29], but once the local states become abundant enough they will act as transporting channels to facilitate electron moving [13,14]. Here the circumstance with higher $N_s$ is similar to the latter. The density of states is remarkably increased to form quasi-continuous transport levels below $E_c$, and these levels can undertake the function of electron conduction, leading to the decrease of resistance $R_s$ in $TiO_2$ film mentioned above.

In Fig. 6, dark current onset potentials for both DSSCs are actually the same under negative bias ($I_3^-$ is reduced to $I^-$ at the $TiO_2$ photoanode), suggesting that the conduction band edge $E_c$ of modified photoanode remains its previous energy level as the normal one. Therefore the positive $E_c$ movement, which thermodynamically promoted the electron injection from activated sensitizer to $TiO_2$ [15,16], should be absent here. Furthermore, the entire group of films treated with different HCl concentration show enhanced currents under negative and positive bias. The enhancement for both current directions is consistent with the conclusion of decreased $R_s$ and $R_2$ in the film and at the $TiO_2$/dye/electrolyte interface.

It should also be noted that the electrolyte used in present study contains $Li^+$ ions, but the better performance

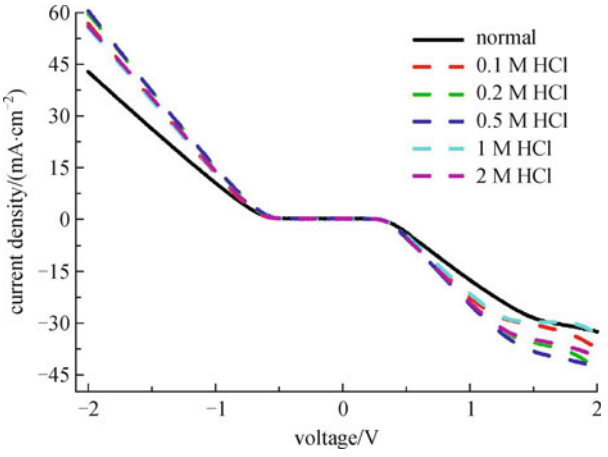


**Fig. 6** Dark current with applied potential for normal (solid line) and HCl treated (dash line) DSSCs with different HCl concentrations

in treated sample is still obtained. Because the HCl treatment is implemented ahead of the DSSC assembly, hydroxyl groups can take up the anchoring sites on $TiO_2$ surface before the $Li^+$ ions intercalation into the film. This advantage accommodates the present modification method in more universal conditions for practical utilization. Furthermore, the conducting electronic states addressed here probably also account for the improved cell performance in $TiCl_4$ treated $TiO_2$ photoanode, which can be considered as effects of nanoparticle surface by both HCl treatment and $TiCl_4$ hydrolysis together.

## 4 Conclusions

We have confirmed the beneficial effect on current density and efficiency of HCl modified DSSCs. The physical origin of the current enhancement is proved to be hydroxyl group induced transporting states created by HCl modification. Distributed below the conduction band edge with a higher density of states, these new surface states are dynamically advantageous for electron injection and transportation due to its large capacitance characteristic for carriers. At the same time $Li^+$ ion is no longer a problem for the functionality of the transporting states, extending the choices of electrolyte. We believe the above conclusions would provide new schemes of modulations to electronic states for optimizing the performance of DSSCs in the future.

**Acknowledgements** This work was supported by the National Natural Science Foundation of China (Grant Nos. 20725311, 20673141, 20703063, 20873178, and 20721140647), the Major State Basic Research Development Program of China (No. 2006CB202606), the National High Technology Research and Development Program of China (No. 2006AA03Z341), and the 100-Talents Project of Chinese Academy of Sciences and Foundation of the Chinese Academy of Sciences (Nos. KJCX2-YW-W27, KGCX2-YW-386-1, and KGCX2-YW-363).

## References

1. O'Regan B, Grätzel M. A low-cost, high-efficiency solar-cell based on dye-sensitized colloidal $TiO_2$ films. Nature, 1991, 353(6346): 737–740
2. Könenkamp R, Henninger R, Hoyer P. Photocarrier transport in colloidal $TiO_2$ films. Journal of Physical Chemistry, 1993, 97(28): 7328–7330
3. Schlichthörl G, Huang S Y, Sprague J, Frank A J. Band edge movement and recombination kinetics in dye-sensitized nanocrystalline $TiO_2$ solar cells: A study by intensity modulated photovoltage spectroscopy. Journal of Physical Chemistry B, 1997, 101(41): 8141–8155
4. Tennakone K, Kumara G R R A, Kottegoda I R M, Perera V P S. An efficient dye-sensitized photoelectrochemical solar cell made from oxides of tin and zinc. Chemical Communications, 1999, (1): 15–16
5. Kambili A, Walker A B, Qiu F L, Fisher A C, Savin A D, Peter L M. Electron transport in the dye sensitized nanocrystalline cell. Physics E, Low-Dimensional Systems and Nanostructures, 2002, 14(1–2): 203–209
6. Meng Q B, Takahashi K, Zhang X T, Sutanto I, Rao T N, Sato O, Fujishima A, Watanabe H, Nakamori T, Uragami M. Fabrication of an efficient solid-state dye-sensitized solar cell. Langmuir, 2003, 19 (9): 3572–3574
7. Shen Q, Toyoda T. Studies of optical absorption and electron transport in nanocrystalline $TiO_2$ electrodes. Thin Solid Films, 2003, 438–439: 167–170
8. Bisquert J, Vikhrenko V S. Interpretation of the time constants measured by kinetic techniques in nanostructured semiconductor electrodes and dye-sensitized solar cells. Journal of Physical Chemistry B, 2004, 108(7): 2313–2322
9. Boschloo G, Hagfeldt A. Activation energy of electron transport in dye-sensitized $TiO_2$ solar cells. Journal of Physical Chemistry B, 2005, 109(24): 12093–12098
10. Rühle S, Dittrich T. Investigation of the electric field in $TiO_2$/FTO junctions used in dye-sensitized solar cells by photocurrent transients. Journal of Physical Chemistry B, 2005, 109(19): 9522–9526
11. Siegers C, Olàh B, Würfel U, Hohl-Ebinger J, Hinsch A, Haag R. Donor-acceptor-functionalized polymers for efficient light harvesting in the dye solar cell. Solar Energy Materials and Solar Cells, 2009, 93(5): 552–563
12. Ferrere S, Gregg B A. Large increases in photocurrents and solar conversion efficiencies by UV illumination of dye sensitized solar cells. Journal of Physical Chemistry B, 2001, 105(32): 7602–7605
13. Gregg B A, Chen S G, Ferrere S. Enhanced dye-sensitized photoconversion efficiency via reversible production of UV-induced surface states in mesoporous $TiO_2$. Journal of Physical Chemistry B, 2003, 107(13): 3019–3029
14. Wang Q, Zhang Z, Zakeeruddin S M, Grätzel M. Enhancement of the performance of dye-sensitized solar cell by formation of shallow transport levels under visible light illumination. Journal of Physical Chemistry C, 2008, 112(17): 7084–7092
15. Wang Z S, Li F Y, Huang C H. Photocurrent enhancement of hemicyanine dyes containing RSO3- group through treating $TiO_2$ films with hydrochloric acid. Journal of Physical Chemistry B,

2001, 105(38): 9210–9217

16. Wang Z S, Yamaguchi T, Sugihara H, Arakawa H. Significant efficiency improvement of the black dye-sensitized solar cell through protonation of $TiO_2$ films. Langmuir, 2005, 21(10): 4272–4276
17. Park D W, Park K H, Lee J W, Hwang K J, Choi Y K. Hydrochloric acid treatment of $TiO_2$ electrode for quasi-solid-state dye-sensitized solar cells. Journal of Nanoscience and Nanotechnology, 2007, 7 (11): 3722–3726
18. Jung H S, Lee J K, Lee S, Hong K S, Shin H. Acid adsorption on $TiO_2$ nanoparticles - An electrochemical properties study. Journal of Physical Chemistry C, 2008, 112(22): 8476–8480
19. Kay A, Grätzel M. Dye-sensitized core-shell nanocrystals: Improved efficiency of mesoporous tin oxide electrodes coated with a thin layer of an insulating oxide. Chemistry of Materials, 2002, 14(7): 2930–2935
20. Palomares E, Clifford J N, Haque S A, Lutz T, Durrant J R. Control of charge recombination dynamics in dye sensitized solar cells by the use of conformally deposited metal oxide blocking layers. Journal of the American Chemical Society, 2003, 125(2): 475–482
21. Liu X Z, Huang Z, Li K X, Li H, Li D M, Chen L Q, Meng Q B. Recombination reduction in dye-sensitized solar cells by screen-printed $TiO_2$ underlayers. Chinese Physics Letters, 2006, 23(9): 2606–2608 (in Chinese)
22. Lee S, Kim J Y, Youn S H, Park M, Hong K S, Jung H S, Lee J K, Shin H. Preparation of a nanoporous $CaCO_3$-coated $TiO_2$ electrode and its application to a dye-sensitized solar cell. Langmuir, 2007, 23 (23): 11907–11910
23. Zaban A, Aruna S T, Tirosh S, Gregg B A, Mastai Y. The effect of the preparation condition of $TiO_2$ colloids on their surface structures. Journal of Physical Chemistry B, 2000, 104(17): 4130–4133
24. Zhang D, Downing J A, Knorr F J, McHale J L. Room-temperature preparation of nanocrystalline $TiO_2$ films and the influence of surface properties on dye-sensitized solar energy conversion. Journal of Physical Chemistry B, 2006, 110(43): 21890–21898
25. Longo C, Nogueira A F, De Paoli M A, Cachet H. Solid-state and flexible dye-sensitized $TiO_2$ solar cells: a study by electrochemical impedance spectroscopy. Journal of Physical Chemistry B, 2002, 106(23): 5925–5930
26. Han L, Koide N, Chiba Y, Mitate T. Modeling of an equivalent circuit for dye-sensitized solar cells. Applied Physics Letters, 2004, 84(13): 2433–2435
27. Wang Q, Ito S, Grätzel M, Santiago F F, Seró I M, Bisquert J, Bessho T. Imai Hachiro. Characteristics of high efficiency dye-sensitized solar cells. Journal of Physical Chemistry B, 2006, 110 (50): 25210–25221
28. Nelson J. Continuous-time random-walk model of electron transport in nanocrystalline $TiO_2$ electrodes. Physical Review B: Condensed Matter and Materials Physics, 1999, 59(23): 15374–15380
29. Bisquert J, Cahen D, Hodes G, Rühle S, Zaban A. Physical chemical principles of photovoltaic conversion with nanoparticulate, mesoporous dye-sensitized solar cells. Journal of Physical Chemistry B, 2004, 108(24): 8106–8118